WILEY-VCH

Direct Evidence of Ultrafast Energy Delocalization Between Optically Hybridized J-Aggregates in a Strongly Coupled Microcavity

Mattia Russo, Kyriacos Georgiou, Armando Genco, Simone De Liberato, Giulio Cerullo, David G. Lidzey, Andreas Othonos, Margherita Maiuri, Tersilla Virgili**

M. Russo, A. Genco, G. Cerullo, M. Maiuri
Dipartimento di Fisica, Politecnico di Milano, Piazza Leonardo da Vinci 32, Milano Italy.
E-mail: margherita.maiuri@polimi.it

M. Russo, S. De Liberato, G. Cerullo, T. Virgili
Istituto di Fotonica e Nanotecnologie – Consiglio Nazionale delle Ricerche (CNR), Piazza Leonardo da Vinci 32, Milano Italy
E-mail: tersilla.virgili@cnr.it

K. Georgiou, A. Othonos
Department of Physics, Laboratory of Ultrafast Science, University of Cyprus, P.O. Box 20537, Nicosia 1678, Cyprus

D. G. Lidzey
Department of Physics and Astronomy, University of Sheffield, Hicks Building, Hounsfield Road, Sheffield S3 7RH, UK

S. De Liberato
School of Physics and Astronomy, University of Southampton, Southampton SO17 1BJ, UK

Keywords: Strong coupling, Energy delocalization, 2D Spectroscopy, Polariton states, organic microcavities

ABSTRACT

Strong coupling between light and matter in a microcavity can produce quasi-particle states termed cavity-polaritons. In cavity architectures containing more than one excitonic species, the photon mode can simultaneously couple to the different excitons, generating new 'hybrid-polariton' states. It has been demonstrated that such hybrid polariton states can energetically connect different molecular species, even when their intermolecular distance is much larger than the Förster transfer radius. Here, we unveil this mechanism and observe in the time domain energy delocalization in a strongly coupled cavity containing two layers of donor and acceptor molecules, separated by an inert spacer layer of 2 μm thickness. We use two-dimensional electronic spectroscopy, a technique that provides simultaneously high spectral and temporal resolution, to probe the dynamics of the energy flow processes following ultra-fast excitation. We show that energy is almost instantaneously delocalized among the polariton states, providing a direct connection between very highly separated donor and acceptor molecules. Our results are of potential significance for light-harvesting devices, optoelectronics and bio-photonic systems.

1. Introduction

Optically active materials placed inside microcavities can experience enhanced light-matter interactions and, under certain conditions, form hybrid quasiparticles called polaritons[1]. In the so-called strong coupling regime, light and matter reversibly exchange energy, with the newly formed polariton states being described by a linear quantum superposition of cavity photons and matter excitations[2]. Owing to their unique properties and the wealth of phenomena they can induce, polaritons have long been of great interest [3-7]. Organic-polaritons are characterized by an enhanced stability at room temperature, stemming from the high binding energy of Frenkel excitons in organic semiconducting materials[8,9]. Therefore, they have been used as testbeds for studies of fundamental physics without the necessity of cooling to cryogenic temperatures[10-13]. Recent experimental and theoretical studies have shown that, apart from non-linear polariton many-body phenomena observed under intense excitation conditions[14-19], the photophysical functionalities of organic materials could potentially[20,21] be altered through their hybridization with cavity photons in the low-excitation regime[22-26], or even in the complete absence of optical excitation[27-29].

By strongly coupling more than one excitonic resonance to the same confined photonic mode, new eigenstates emerge that are formally described as a mixture of the photon and of the different excitons. If the different excitons are located in distant materials inside the microcavity,

the polaritonic coupling allows long-range energy transfer (ET) between spatially separated donor-acceptor molecular aggregates that are hybridized through their mutual coupling to the same optical mode[30-33]. Importantly, unlike other nonradiative dipole-dipole ET mechanisms, polariton-mediated energy transfer is not limited by the separation between donor and acceptor molecular species. Rather, the large exciton oscillator strengths permit a coupling between molecules having different electronic energy transitions[33] over mesoscopic distances of several microns[34]. We note that other physical properties – such as cavity photon lifetime and exciton broadening – also affect the hybridization of the excitonic states and can modify ET processes.

Theoretical work by Sánchez Muñoz and coworkers[35] has demonstrated that the temporal evolution of the energy flow in such coupled systems depends on the degree of hybridization between the various polariton states. Indeed, narrow, and spectrally well-separated excitonic transitions lead to polariton states having a greater degree of hybridization, with the excitonic contribution being (in some cases) comparable to that of the cavity photon. This results in polaritons having a wavefunction that is spatially delocalized throughout the entire microcavity, enabling an ultrafast energy redistribution among polariton-states.

Ultrafast spectroscopy is a powerful tool to probe carrier dynamics and energy transfer processes in materials and devices[,33,36-43]. However, when applied to study polariton relaxation dynamics, ultrafast experiments become very challenging to perform and to interpret[44] due to two factors: (i) the ultrashort lifetime of the cavity photons, typically of the order of few tens of femtoseconds, depending on the cavity Q factor, and (ii) the ultrafast polariton decay, mainly dominated by relaxation towards dark states. These are formalized by the Tavis-Cummings model [45] and are also understood as resulting from uncoupled excitons that exist in a 'reservoir' of states [26,46-48].

To probe timescales on which polaritons are coherent (i.e. when the wavefunctions of excitons and photons are inseparably mixed[26,36,44]), it is necessary to use ultra-short laser pulses whose duration is shorter than the lifetime of polaritons. Two-dimensional electronic spectroscopy (2DES)[49,50] is a powerful technique which allows one to achieve high temporal resolution while, at the same time, providing high spectral resolution over the excitation frequency. Three delayed laser pulses are used in 2DES, with the excitation energy axis being obtained by performing a Fourier transform of the signal with respect to the coherence time t_1 between the first two pump pulses. The temporal evolution of the system is then obtained by scanning the delay t_2 (waiting time) between the second and the third pulse, the latter acting as a probe.

Recently 2DES has been applied to study ultrafast dynamics in a few microcavity structures[51,52,53]. Notably, Son and coworkers [53] evidenced an energy cascade process in donor-acceptor cavities containing films of semiconducting carbon nanotubes distanced by about 150 nm, with a transfer from the highest- to the lowest-energy polariton state occurring in 200 fs. However, in the limit of narrow excitonic transitions and significant photonic components of the polariton states, they predicted the upper-to-lower energy relaxation to become quasi-instantaneous. This was not observed due to the largely excitonic nature of the polaritons formed in the cavities studied. Therefore, forming highly hybridized polaritons and showing experimentally the inherent instantaneous energy redistribution over mesoscopic distances, remains a challenge.

In this work, we report the fabrication of a microcavity containing two thin films of J-aggregated organic semiconductors (named TDBC and NK2707), where the J-aggregate layers are separated by a micron-thick, inert and transparent spacer. Here, strong coupling to the cavity photon-mode results in the formation of a series of hybrid-polariton states. In this system, excitonic transitions are sufficiently narrow and spectrally separated, leading to hybridized polariton states containing a significant photon component, as well as a mixture of the two excitons.

We use 2DES to characterize the energy flow mechanisms between the polariton states both temporally and spectrally. Our measurements provide direct evidence of ultrafast mesoscopic energy delocalization and coupling between the molecules in the different layers driven by polariton hybridization. Our results agree with theoretical predictions for systems in which polariton states have strong photon character. Our findings have relevance for the development of advanced optoelectronic devices exploiting polaritons to enhance energy transfer, and for the understanding of energy-harvesting processes in bio-photonic architectures [54,55].

2. Results

As the active materials in our experiments, we have used the molecular dyes 5,6 dichloro-2-[[5,6-dichloro-1-ethyl-3-(4-sulphobutyl)- benzimidazol-2-ylidene]-propenyl]-1-ethyl-3-(4-sulphobutyl)-benzimidazolium hydroxide, sodium salt, inner salt (TDBC) and 5-chloro-2-[3-[5-chloro-3-(3-sulphopropyl- 2(3H)-benzothiazolylidene]-2-methyl-1-propenyl]-3-(3-sulphopropyl)- benzothiazolium hydroxide, inner salt, compound with triethylamine (NK2707). These were dispersed into a transparent polymeric matrix (gelatine) and cast into

thin films by spin-coating. Upon aggregation, such dyes form J-aggregates which result from phase-separation and subsequent crystallization / self-assembly of the cyanine dyes placed in a matrix[31]. In these aggregates electronic coupling between molecular dipoles creates delocalized, red-shifted and spectrally narrowed excitonic states. We have used a sequential spin-coating technique to create a multilayer structure in which J-aggregated TDBC and NK2707 dye layers were physically separated from one another using a 2μm optically transparent polystyrene (PS) spacer layer. The mesoscopic thickness of the PS spacer layer, which is much larger than the Förster radius, prevents direct ET between the J-aggregated dyes. Figure 1a shows a schematic of the multilayer film, together with the chemical structure and the steady state absorption of both J-aggregated dyes. The TDBC J-aggregate (highlighted in blue) has an absorption peak at 2.13eV, while the absorption of the NK2707 aggregate (plotted in red) peaks at lower energy (1.96eV) together with a broad shoulder that peaks around 2.13eV.

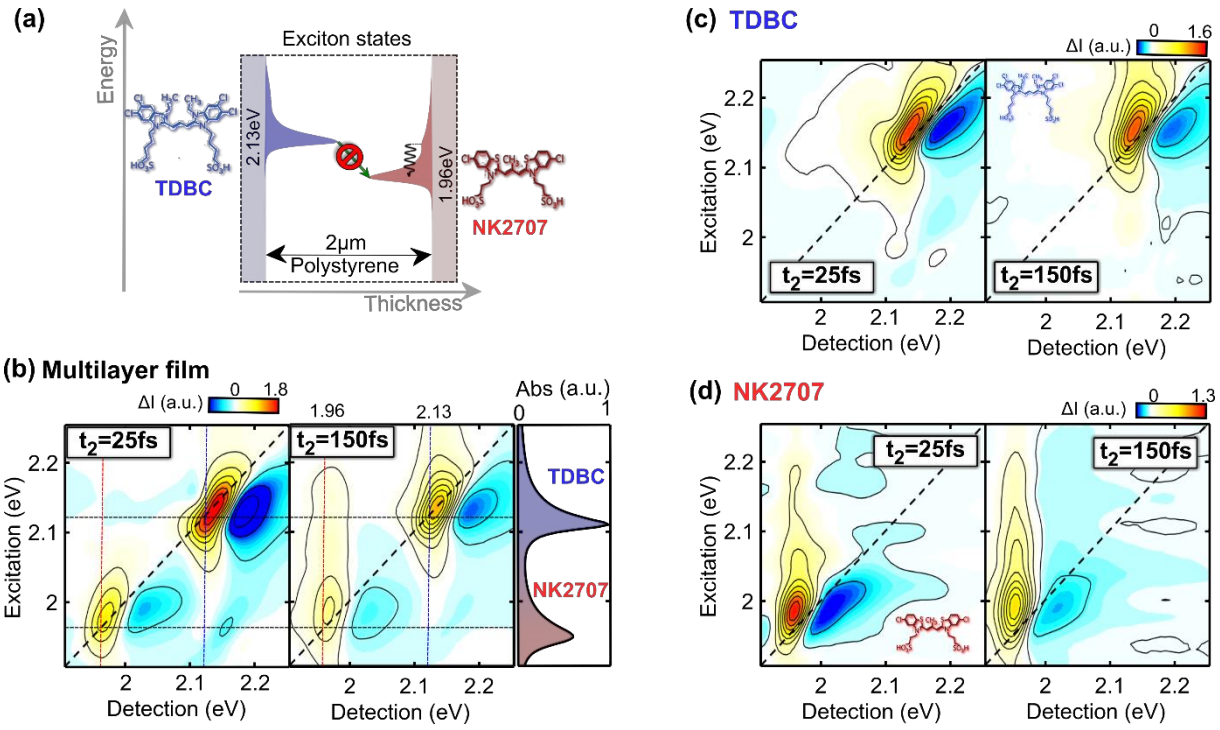

Figure 1. (a) Schematic representation of the multilayer film accompanied by the steady state absorption and molecular structure of the NK2707 (red) and TDBC (blue). Here the black wavy arrow corresponds to an intramolecular energy relaxation process in NK2707. (b) Steady state absorption spectrum (right) of the non-cavity control film and purely absorptive 2DES maps at t_2 = 25fs (left) and 150fs (middle), where the spectral positions of the TDBC and NK2707 exciton states are identified using horizontal and vertical dashed lines. (c) Purely absorptive

2DES maps of a TDBC single film at t_2 = 25fs (left) and 150fs (right). (d) Purely absorptive 2DES maps of a NK2707 single film at t_2 =25fs (left) and 150fs (right).

We first use broadband 2DES to demonstrate the absence of direct ET between the two J-aggregated dyes in the multilayer film. Broadband laser pulses, spanning from 1.88 eV to 2.25 eV, temporally compressed to 15 fs, were used to pump and probe the excitonic population of the two J-aggregates. The 2DES apparatus is described in the Methods section. Figure 1b shows 2DES maps of the multilayer recorded at waiting times t_2 = 25 fs and 150 fs, together with steady state absorption spectrum in the right panel.

At t_2 = 25 fs, the 2DES map is composed of two diagonal signals in correspondence with the absorption peaks of the two species, with no cross peaks being evident. Each of these signals contains a positive peak, corresponding to the ground state bleaching (GSB) and stimulated emission (SE) of the excitonic transition, and a negative peak at slightly higher photon energies, corresponding to a photoinduced absorption (PA) due to the transition from exciton states to energetically higher excited states [56,57]. At t_2 = 150 fs, we observe the formation of a positive cross peak that corresponds to excitation over the spectral range covering 2eV to 2.2eV and detection at 1.96eV (the absorption peak of NK2707). This peak could either represent direct ET from TDBC (the donor) to NK2707 (the acceptor) or a simple internal relaxation process within NK2707, in which excitons scatter from higher to lower energy states. To determine the nature of this process, 2DES was performed on films of pure TDBC and NK2707 with the same thickness and concentration as used in the multilayer film.

Figure 1c shows the 2DES maps of a TDBC thin film at t_2 = 25 fs and 150 fs. At both time delays, a diagonal peak reflecting the steady-state absorption is observed. The main difference between the two 2DES maps relates to the lineshape of the diagonal peaks; specifically, the peak observed at t_2 = 25 fs has an elliptical shape and is stretched along the diagonal. At t_2 = 150 fs this feature has broadened along the anti-diagonal direction. This process is typical in molecular materials, and results from spectral diffusion effects and loss of excitation memory[58].

Figure 1d shows 2DES maps of a NK2707 film at t_2 = 25 fs and 150 fs. Here the maps are dominated by an intense absorption peak at 1.96eV that is located along the diagonal line. We observe the build-up of a cross peak at 1.96eV following excitation in the spectral range 2eV to 2.2 eV. We attribute such peaks to an internal conversion process from a higher to a lower energy state at 1.96eV. Such signals are comparable in magnitude with the cross peaks observed in the multilayer film, implying that there is no direct ET process between the donor

(TDBC) and the acceptor (NK2707) species. Rather, the cross peaks observed in the multilayer films result from an internal conversion mechanism within the NK2707 (see wavy black arrow in Figure 1a). The dynamics of these cross peaks are compared in Figure S1, and no difference is observed between the multilayer film and the film containing NK2707 alone.

We now discuss the ultrafast optical response of the multilayer film when its components are strongly coupled to the optical microcavity. The linear optical properties of this structure have previously been discussed in detail by Georgiou et al.[34], and it has been demonstrated that the excitonic states of both TDBC and NK2707 are simultaneously strongly coupled to a series of cavity modes[34]. As a result of this coupling, several polariton branches are observed that undergo simultaneous anti-crossing.

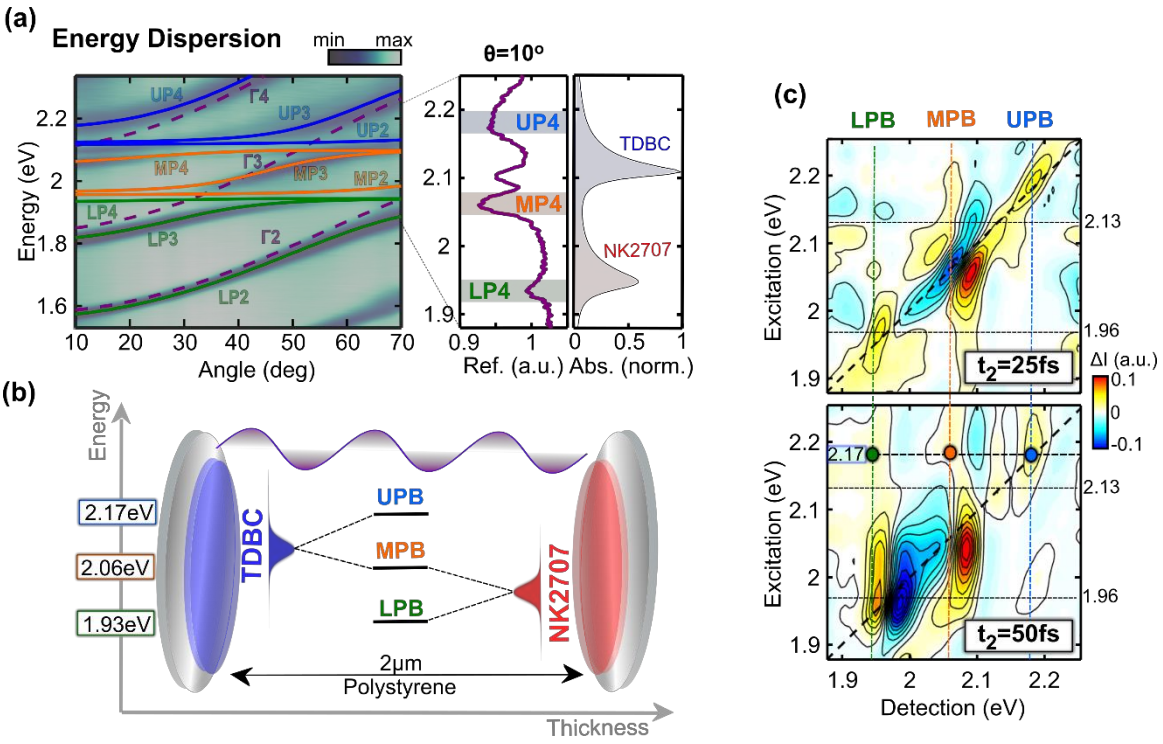

Figure 2. (a) Energy dispersion map of the microcavity where the coloured lines indicate the Upper (blue), Middle (orange) and Lower (green) polariton branches calculated using a coupled oscillator model. We also identify the TDBC and NK2707 exciton states and the cavity modes (violet dashed lines). On the right side, there is a zoom in of the reflectivity map at 10° from 1.88eV to 2.25 eV along the energy axis, which corresponds to the region probed in the 2DES experiment. (b) Energy level scheme of the organic microcavity in the strong coupling regime where the energy axis is labelled with the energies of the polariton states; UPB at 2.17eV, MPB at 2.06eV and LPB at 1.93eV. The black dashed lines mark the dominant excitonic contributions to each polariton state. (c) Purely absorptive 2DES spectra at t_2 = 25fs (top) and

50fs (bottom). The dashed lines along the detection axis represent the position of the polariton states and the dashed lines along the excitation axis correspond to the excitonic states of NK2707 (1.96eV) and TDBC (2.13eV).

Figure 2a shows angle-dependent white-light optical reflectivity measurements of the cavity to map out the dispersion of the polariton branches over an angular range between 10° and 70°, as previously measured [34]. Due to the substantial thickness of the cavity spacer layer (leading to a significant optical cavity path-length), multiple cavity modes are supported (labelled Γ2, Γ3 and Γ4), each of which undergoes anticrossing when they come into resonance with the two molecular species (see absorption spectra shown in the right side of the panel). This ladder of cavity modes results in a series of different polariton modes that we term as upper, middle and lower polaritons (UP, MP, LP). We describe the energy dispersion of these polariton modes using an n-level coupled-oscillator model fit as shown in Figure 2a, with relevant parameters and Hopfield coefficients reported in Supporting Information (Table S1 and Figure S2). The exact photon/exciton character of the different polariton branches is dependent on energetic detuning and angle of observation, however it has been previously shown that for the upper UP and LP the cavity mode is preferentially mixed with a substantial fraction of either TDBC or NK2707, respectively[34]. In contrast, the MP contains an admixture of the cavity mode with both molecular species[34].

Here, we focus on the polariton states covered by the spectrum of our laser (from 1.88eV to 2.25eV) and measurement angle (10°), highlighted in the zoom out of Figure 2a, right panel. It is apparent that there are several polariton states within the measurement window (namely LP4, MP4 and UP3,4). In what follows, we focus our discussion by describing the series of polariton states coupled with photon-mode Γ4. For simplicity, we refer to UP4 (at 2.17 eV) as UPB, MP4 (at 2.06 eV) as MPB and LP4 (at 1.93 eV) at the LPB as sketched in Figure 2b. The rationale to exclude UP3 from our analysis is that in multimode polariton systems, photonic modes exist in a 'decoupled' regime which has been theoretically predicted[59,60] and experimentally observed[61,62]. Thus in our cavity, the various photonic modes are not coupled to each other, and the sets of polariton-states generated (LP, UP and MP) can be treated individually.

Figure 2c shows the 2DES maps obtained for the organic microcavity for 10° incidence angle at t_2 = 25 fs and 50 fs. In this experiment, we pump the cavity using broadband laser pulses and record its transient reflectivity (ΔR). Here, the main polariton contributions to the probe signal are identified via different coloured areas (LPB – green, MP B– orange, UPB –

blue). We identify the energies of the different polariton states via vertical lines in the 2DES maps, with the energy of the uncoupled excitons shown using horizontal lines.

At $t_2 = 25$ fs we observe three diagonal peaks that correspond to transient signals of each polariton state. These peaks have a derivative lineshape with contributions from both negative and positive signals. This effect results from the fact that when an organic exciton-polariton is pumped, the refractive index of the active material and the oscillator strength of the exciton peak are reduced [17, 63]. This causes a contraction of the Rabi splitting and a near instantaneous blue/red-shift of the polariton states, resulting in a derivative lineshape of the 2DES signal. At $t_2 = 50$ fs we find that the 2DES map includes cross peaks detected at MPB and LPB energies as a result of excitation of the UPB state, marked in the 2DES map with orange (MPB) and green (LPB) circles. Such signals are a signature of a transfer mechanism between the polariton states and, consequently, between the TDBC and NK2707 molecules.

3. Discussion

In this section, we investigate possible energy transfer pathways between the donor and acceptor dyes assisted by the polariton states via an analysis of the dynamics of the cross peaks, which represent transient absorption signal of the system detected at an energy that is different with respect to the excitation energy. Figure 3a shows a 2DES map of the organic microcavity at $t_2 = 100$ fs; here the horizontal dashed lines correspond to excitation of the following states: UPB (2.17 eV), TDBC exciton (2.13 eV) and NK2707 exciton (1.96 eV). Figures 3b, c and d plot the measured dynamics of the cross peaks identified in panel (a) as a function of the waiting time t_2.

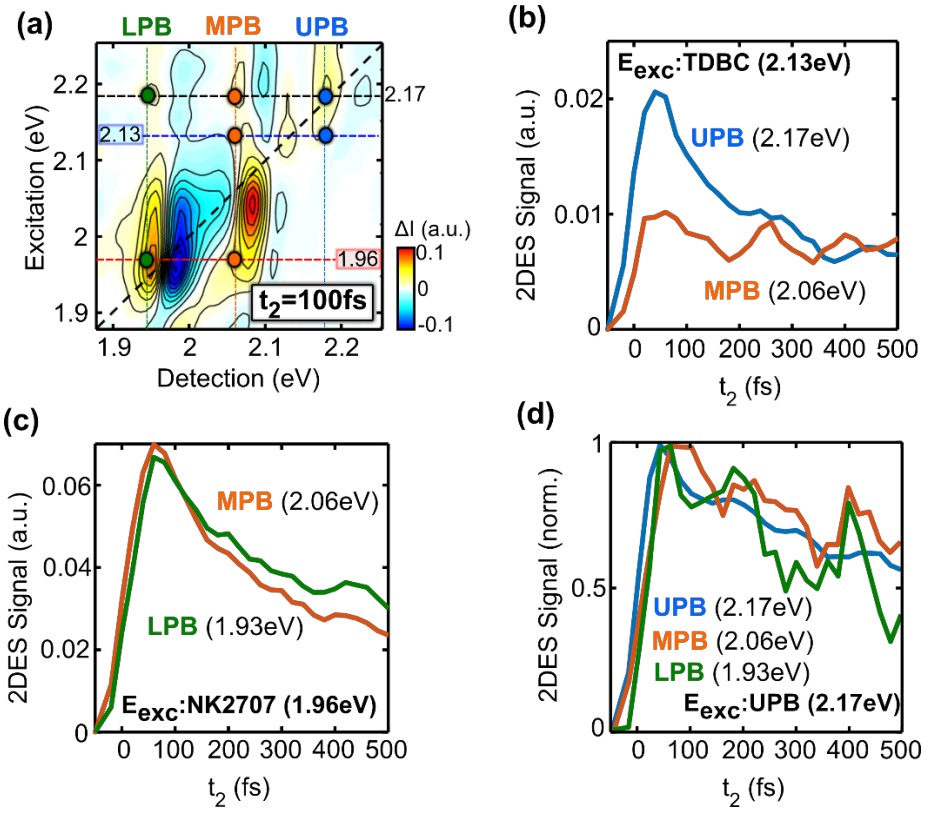

Figure 3. 2DES time traces: (a) Purely absorptive 2D map at $t_2 = 100$fs used to highlight specific dynamics at selected excitation/detection energies. (b) t_2 traces obtained by exciting the TDBC exciton (2.13eV) and detecting the UPB (2.17eV, blue) and MPB (2.06eV, orange) states. (c) t_2 traces obtained by exciting the NK2707 exciton (1.96eV) and detecting the MPB (2.06eV, orange) and LPB (1.93eV, green) states. (d) normalized t_2 traces obtained by exciting the UPB (2.17eV) and detecting the UPB (2.17eV blue), MPB (2.06eV, orange) and LPB (1.93eV, green) states. The dynamics reported in panels (b), (c) and (d) correspond to the points in the 2D map of panel (a) that are emphasized with dashed lines and coloured circles.

We first focus on the polariton cross peaks that result from the excitation of the uncoupled exciton reservoir. This is shown in Figure 3b where we plot dynamics obtained by excitation at 2.13eV (corresponding to the TDBC exciton) and detection of the cross peaks at 2.06eV (MPB, orange) and 2.17eV (UPB, blue). Both dynamics have a rise time comparable with the ≈ 20fs temporal resolution of the experiment. This suggests that once the TDBC reservoir excitons have been created, an immediate coherent coupling to the cavity occurs, resulting in instantaneous bleaching of the UPB and MPB states. After the signal build-up, the dynamics of the two polaritons look very different. In particular, the UPB undergoes a more rapid decay than the MPB, whose transient signal remains nearly constant over the first 500 fs. We ascribe such slow MPB dynamics to the balance between formation and decay mechanisms;

the formation is due to the relaxation from the UPB states, while the decay is due to relaxation to the LPB ground state. It is important to underline that our 2DES data do not allow to completely isolate the contribution of the exciton reservoir, since the linewidths of the excitons are broader with respect to the energy distance between the polariton states. For this reason, our results do not exclude a possible transfer from the UPB to the TDBC exciton reservoir, however they clearly show that the coupling between all the polariton states occurs on an ultrafast time scale.

Figure 3c plots cavity dynamics obtained following excitation at 1.96 eV (corresponding to the NK2707 exciton) and detection at energies corresponding to the cross peaks at 2.06 eV (MPB - orange) and 1.93 eV (LPB - green). We observe a nearly instantaneous rise in the signal, again confirming an immediate coupling with the cavity mode. The subsequent decay of the LPB is comparatively slower than that of the MPB; a result that likely signals a degree of exciton relaxation from the MPB to LPB states. Other possible relaxation pathways include scattering from MPB states to the exciton reservoir which then populate states in the LPB[64-66]. Therefore, the dynamics of LPB states may well be slower than the depopulation of the MPB because this likely involves partial filling of and then depopulation of the exciton reservoir.

Finally, Figure 3d shows normalized cavity dynamics recorded following excitation of the UPB and detected at the diagonal peak at 2.17 eV (UPB, blue) and at the cross peaks 2.06 eV (MPB, orange) and 1.93 eV (LPB, green). As expected, the signal from the UPB diagonal peak forms instantaneously; remarkably, the cross peaks detected at MPB and LPB also undergo a nearly instantaneous rise within the limit of the sub-20-fs experimental temporal resolution. Interestingly, the excitation of the UPB results in a detectable signal from the LPB, which is not visible following the excitation of the higher energy TDBC exciton. This result strongly indicates that our transient responses are completely dominated by the polaritons properties and they cannot be reproduced simply considering the cavity as a filter of the ground- and excited-state excitons populations, as previously reported in different systems[67]. Figure S3 in the Supporting Information compares the unnormalized cross peaks dynamics when exciting the TDBC excitons at 2.13 eV (Figure S3(a)) and the UPB at 2.17 eV (Figure S3(b)). The lack of a cross-peak at the LPB when exciting the TDBC exciton indicates that, on a short timescale, exciton-driven incoherent energy transfer pathways between TDBC and NK2707 are not effective. Moreover, also a direct excitation of the NK2707 at 2.13 or at 2.17 eV does not lead to an appreciable nonlinear signal in the microcavity.

Our measurements allow us to draw two main conclusions: i) coherent coupling occurs between the three polaritons states, however this is not observed following the direct excitation

of the exciton reservoir and ii) the ultrafast formation of the transient signal detected at MPB and LPB energies following the excitation of the UPB suggests that the energy rapidly delocalizes throughout the entire cavity. This coupling drives energy delocalization between the different molecular species, even though they are physically separated by 2μm, a distance much greater than the Förster transfer radius. Note that this process still respects causality, and when using the term instantaneous we implicitly refer to timescales substantially longer than the inverse coupling frequencies between light and matter, which in our case are of the order of the experimental time resolution. We would like to underline that we use the term "energy delocalization" as equivalent to "coherent coupling" or "excitation delocalization" between polariton states. Coherent excitations can be transferred very rapidly between a photon and an exciton in the strong coupling regime (with the transfer rate given by the Rabi frequency). A previously reported example of the importance of fast coherent processes in these systems is the observation of Rabi oscillations in 2D spectroscopy experiments on molecular J-aggregates strongly coupled to a plasmonic grating[68]. Furthermore, very recently Tuomas Pajunpää et al. demonstrated by full quantum dynamics simulations that polariton-assisted exciton population exchange dynamics can occur over a distance of 1 μm between interacting materials[69].

To confirm our data, we performed additional measurements using broader pump and probe pulses, with spectrum spanning 1.77-2.25 eV which also excites the Γ3 cavity mode. Again, we see a very similar phenomenology for the dynamics of the UPB, MPB and LPB (see Figure S4).

To gain further insight into this process, we have simulated the 2DES signal from the cavity using a fully coherent, broadband polaritonic model summarized in the Methods section and in the Supporting Information. The Methods section also discusses justifications and limitations of the theoretical model. Figure 4a (top panel) shows the experimental 2DES data at t_2 = 100 fs limited to the excitation region from 2.13 eV to 2.25 eV to emphasize the cross peaks, with the bottom panel in Figure 4a being a theoretical simulation of the experimental data. While our coherent model is unable to provide quantitative predictions, it reproduces correctly the position of the polariton peaks and their derivative lineshape, validating our interpretation of instantaneous energy delocalization between the different exciton components driven by a single cavity mode. Here, we mark the peaks using coloured circles in panel a, and then plot their normalized simulated dynamics in Figure 4b. Specifically, the dynamics plotted

are generated following simulated excitation at 2.17eV (UPB) and then detection at 2.17eV (blue), 2.06 eV (MPB, orange) and 1.93eV (LPB, green).

Comparing the dynamics calculated from the theoretical model excited at the UPB frequency to measured data in Figure 3d, we can see how the model reproduces some of the early-time features observed in the data, such as the slower rise-time of the signal detected at LPB and MPB frequencies with respect to the UPB. The model fails however to correctly reproduce the evolution of the signal at longer delay times due to its fully coherent nature, conflating populations and coherence lifetimes. This does not allow signal damping to be correctly described as it is visible by the much faster decays predicted by the theory as compared to measured data. We note that in the absence of dephasing, the theoretical model predicts coherent oscillations (see Figure 4b) due to beating between the different polariton modes, not sufficiently clear in the experimental observations, with these oscillations being akin to the Rabi oscillations observable in the time dynamics of strongly coupled systems.

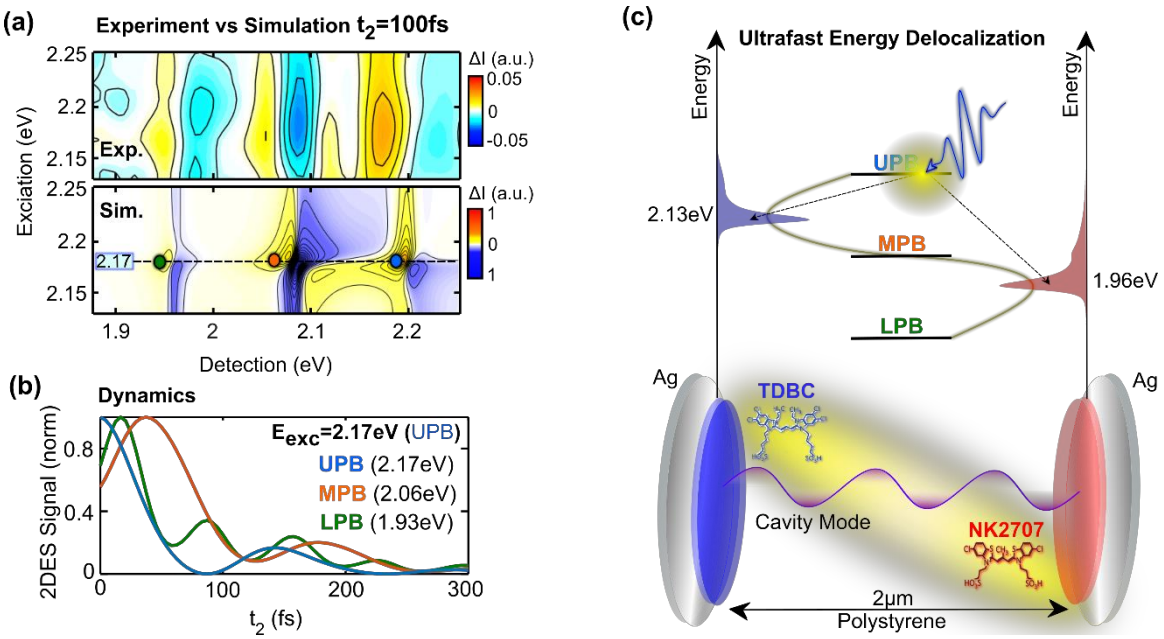

Figure 4. Simulation and model: (a) Experimental data (top) and simulated signal (bottom) purely absorptive 2DES map at t_2=100fs where the excitation axis is cut from 2.13eV to 2.25eV and the detection axis is limited between 1.88eV and 2.25eV. (b) Simulated t_2 traces of the points indicated in the simulated 2DES map reported in part (a). Here such points are obtained by exciting the UPB (2.17eV) and detecting the UPB (2.17eV, blue), MPB (2.06eV, orange) and LPB (1.93eV, green). (c) Deactivation energy level scheme after the excitation of the UPB state where dashed black arrows indicate an ultrafast delocalization of the energy among

exciton and polariton states. The yellow line in the energy level scheme (top) represents the energy path that provides a connection between the TDBC and NK2707.

4. Conclusions

In summary, we exploited the combination of high temporal and spectral resolution of 2DES to reveal the mechanism of long-range ultrafast energy transfer between two dyes in a strongly coupled organic microcavity. We study a multilayer comprised of two thin layers of the J-aggregate dyes TDBC and NK2707 that were spatially separated by a 2μm PS transparent film. Our results show that this system behaves differently when located inside or outside a microcavity. Specifically, when measured outside a cavity, we do not evidence any energy transfer process between the two dyes, a result expected on the basis of the Förster transfer-radius limit. 2DES measurements on the cavity indicate the presence of the polariton states due to the strong coupling and the presence of cross peaks that are formed in a time scale comparable with the temporal resolution of the experiment (20fs). Figure 4c schematically illustrates the cavity system (bottom) and its energy levels (top). Here, we graphically represent the ultrafast energy delocalization over the entire system obtained as a result of the excitation of the UPB state. Specifically, upon excitation of the UPB, energy is coherently delocalized throughout the entire cavity, providing a direct connection between the molecular excitons. Such a mechanism is supported by simulations of the 2DES data obtained using a model that considers interaction of the molecular excitons with a single cavity mode. Despite the fact that our model does not reproduce the amplitude of the various signals, it does allow us to predict the ultrafast formation of the cross peaks and their 2D lineshape. Our results should stimulate the design of innovative optoelectronic devices in which polariton states are exploited to drive efficient energy transfer among coupled chromophores.

5. Experimental Section/Methods

Two-dimensional electronic spectroscopy (2DES): The experimental apparatus used in this work is described in detail elsewhere[70]. Briefly, the broadband laser pulses are generated by a non-collinear optical parametric amplifier (NOPA) pumped by an amplified Ti:Sapphire laser that generates 100-fs pulses at 1 kHz and 800 nm wavelength. The NOPA produces pulses with a 1.88-2.25 eV bandwidth, that are compressed to sub-20-fs duration using a pair of chirped mirrors. In this work, pump and probe laser pulses are frequency degenerate and we use a partially collinear pump-probe geometry in which the first two pulses are collinear and a third probe pulse, acts as local oscillator. The delay time t_1 is controlled using a common-path

birefringent interferometer, the Translating-Wedges-Based Identical pulses encoding System (TWINS) system[71]. In our experiment, t_1 is scanned from -30fs to 250fs. The delay time t_2 is controlled by a standard mechanical translation stage along the probe optical path and is scanned from -250 to 3000 fs. In all the experiments reported, the polarization between the pump and the probe beam was fixed at the magic angle (54.7°). The single-component molecular films and the multilayer film were measured in transmission and excited at a fluence of 45 μJ/cm^2. The organic microcavity however was measured in reflection at an incidence angle of 10° (± 5°) and excited at a fluence of 100μJ/cm^2. The small incidence angle allows to neglect the polarisation dependence of the cavity mode[72].

Control-film and Microcavity Fabrication: J-aggregates NK2707 (supplied by Hayashibara Biochemical) and TDBC (supplied by FEW Chemicals GmbH) were dissolved at a concentration of 5% and 10% by weight in a deionized water / gelatine solution (20 mg mL^{-1}), respectively. J-aggregate / gelatine solutions were held at a temperature of 65°C before 100 μL of solution was used to spin-cast thin films. PS (supplied by Sigma-Aldrich) having a molecular weight of Mw ~ 350,000 was dissolved in toluene at a concentration of 100 mg mL^{-1} and spin-casted using 200 μL of solution held at room temperature. Control over the thickness of the various thin layers was achieved by changing the rotation speed of the substrate during spin-casting, and was determined with a Bruker Dektak XT profilometer.

An Ångstrom Engineering thermal evaporator was used to evaporate the microcavity Ag mirrors. The Ag deposition rate was maintained between 0.5 and 1 Å/s^{-1} with the sample chamber being held at a base pressure of 2 × 10^{-6} mbar. The bottom and top mirrors had a thickness of 200 nm (fully reflective) and 34 nm (semi-transparent), respectively. The organic multilayers were fabricated by subsequently spin-casting the various J-aggregate / gelatine and PS layers, as described above.

Theoretical model: General quantum theories of 2DES that are able to provide quantitative predictions need to consider both coherent and incoherent processes on the same footing[73]. This is due to the potential proximity of the timescales involved in the two kinds of processes in ultrafast optical experiments. Due to the inherent complexity of the many-body coupling between bright and dark states in polaritonic systems, alternative approaches are used to confirm qualitative interpretation of experimental data[74]. If delay times substantially longer than the cavity lifetime are considered, we can use a fully incoherent theory in which the oscillations

of the short-lived polaritonic states interact nonlinearly with an incoherent reservoir of dark excitons. In our case a cavity lifetime of ~164 fs is well resolved using our available temporal resolution. We thus used a complementary, fully coherent polaritonic model. In the same spirit we make a broadband approximation in which we neglect the temporal overlap between successive pulses. Note that for waiting times comparable or longer than the excitation lifetimes, the predictions of the fully coherent model regarding the absolute value of the signal intensity will necessarily degrade due to the absence of dark states. In other terms, in our theory populations and coherences have the same lifetime.

As described in more details in the Supporting Information, we describe the pumped system using the non-Hermitian, non-linear Hamiltonian $H = \sum_q H_L(q) + \sum_{q,q',q''} H_{NL}(q,q',q'')$, where the first term models the linear, lossy, and pumped system, and the second the cubic nonlinear interactions between cavity photons, TDBC excitons, and NK2707 excitons. We can solve $H_L(q)$ by writing the time evolution of the photon and exciton fields under the effect of the external pump and of their mutual interactions and then inject these into $H_{NL}(q,q',q'')$ to calculate the induced third-order polarization. Such simulations are performed in the broadband approximation, that is considering instantaneous pulses. This explains the non-zero value of the pumped mode obtained at $t_2 = 0$. The linear parameters required for the simulations are determined from the experimental steady state absorption spectrum of thin films containing each type of J-aggregated dye (see Figure 1) with the frequencies and linewidths of the different modes obtained by fitting the coupled resonances. The non-linear coefficients of the excitons have been calculated from the respective molecular densities using the Agranovich-Toshich transformation[75], while the non-resonant non-linear coefficient of the photonic field, corresponding to the transparent polystyrene spacer-layer, has been taken from the literature[76]. The dynamical evolution of the system can then be written as a nonlinear wave equation coupling the cavity mode with the two excitonic resonances, and analytically solved in the broadband limit for the intensity of the photonic component which is proportional to the 2DES measured signal. More explicit calculations, as well the list of parameters used are given in the Supporting Information.

Supporting Information

Supporting Information is available from the Wiley Online Library or from the author.

Acknowledgements

S.D.L. acknowledges funding from the Leverhulme Trust (grant RPG-2022-037). D.G.L. and K.G. thank the U.K. EPSRC for funding via the Programme Grant 'Hybrid Polaritonics' (EP/M025330/1). K.G. and A.O. acknowledge support from the University of Cyprus through the postdoctoral fellowship program 'Onisilos' M.M. acknowledges funding from the European Union (ERC-StG, ULYSSES, 101077181). Views and opinions expressed are however those of the author(s) only and do not necessarily reflect those of the European Union or the European Research Council. Neither the European Union nor the granting authority can be held responsible for them. M.M and G.C. acknowledge financial support by the European Union's NextGenerationEU Programme with the I-PHOQS Infrastructure [IR0000016, ID D2B8D520, CUP B53C22001750006] "Integrated infrastructure initiative in Photonic and Quantum Sciences.

Received: ((will be filled in by the editorial staff))
Revised: ((will be filled in by the editorial staff))
Published online: ((will be filled in by the editorial staff))

References

[1] C. Weisbuch, M. Nishioka, A. Ishikawa, Y. Arakawa, *Phys. Rev. Lett.* **1992**, *69*, 3314–3317.

[2] A. V. Kavokin, J. J. Baumberg, G. Malpuech, F. P. Laussy, *Microcavities*, Second Edi Oxford Univ. Press, UK **2017**.

[3] P. G. Savvidis, J. J. Baumberg, R. M. Stevenson, M. S. Skolnick, D. M. Whittaker, and J. S. Roberts, *Phys. Rev. Lett.* **2000**, *84*, 1547–1550.

[4] J. Kasprzak, M. Richard, S. Kundermann, A. Baas, P. Jeambrun, J. M. J. Keeling, F. M. Marchetti, M. H. Szymańska, R. André, J. L. Staehli, V. Savona, P. B. Littlewood, B. Deveaud and Le Si Dang, *Nature* **2006**, *443*, 409–414.

[5] K. G. Lagoudakis, M. Wouters, M. Richard, A. Baas, I. Carusotto, R. André, Le Si Dang and B. Deveaud-Plédran, *Nat. Phys.* **2008**, *4*, 706–710.

[6] N. G. Berloff, M. Silva, K. Kalinin, A. Askitopoulos, J. D. Töpfer, P. Cilibrizzi, W. Langbein and P. G. Lagoudakis, *Nat. Mater.* **2017** *16*, 1120–1126.

[7] S. Klembt, T. H. Harder, O. A. Egorov, K. Winkler, R. Ge, M. A. Bandres, M. Emmerling, L. Worschech, T. C. H. Liew, M. Segev, C. Schneider and S. Höfling, *Nature* **2018**, *562*, 552–556.

[8] D. G. Lidzey, D. D. C. Bradley, M. S. Skolnick, T. Virgili, S. Walker and D. M. Whittaker, *Lett. to Nat.* **1998** *395*, 53–55.

[9] Z. Jiang, A. Ren, Y. Yan, J. Yao, Y. S. Zhao, *Adv. Mater*. **2022**, *34*, 2106095.

[10] J. D. Plumhof, T. Stoeferle, L. Mai, U. Scherf, R. F. Mahrt, *Nat. Mater.* **2014**, *13*, 247–252.

[11] K. S. Daskalakis, S. A. Maier, R. Murray, S. Kéna-cohen, *Nat. Mater.* **2014**, *13*, 271–278.

[12] G. Lerario, D. Ballarini, A. Fieramosca, A. Cannavale, A. Genco, F. Mangione, S. Gambino, L. Dominici, M. De Giorgi, G. Gigli and D. *Light Sci. Appl*. **2017**, *6*, e16212.

[13] R. Jayaprakash, C. E. Whittaker, K. Georgiou, O. S. Game, K. E. McGhee, D. M. Coles, and D. G. Lidzey, *ACS Photonics* **2020**, *7*, 2273–2281.

[14] C. P. Dietrich, A. Steude, L. Tropf, M. Schubert, N. M. Kronenberg, K. Ostermann, S. Höfling, and M. C. Gather, *Sci. Adv.* **2016**, *2*, e1600666.

[15] T. Cookson, K. Georgiou, A. Zasedatelev, R. T. Grant, T. Virgili, M. Cavazzini, F. Galeotti, C. Clark, N. G. Berloff, D. G. Lidzey, P. G. Lagoudakis, Adv. *Opt. Mater.* **2017**, *5*, 1700203.

[16] A. Putintsev, A. Zasedatelev, K. E. McGhee, T. Cookson, K. Georgiou, D. Sannikov, D. G. Lidzey, P. G. Lagoudakis, *Appl. Phys. Lett.* **2020**, *117*, 123302.

[17] T. Yagarof, D. Sannikov, A. Zasedatelev, K. Georgiou, A. Baranikov, O. Kyriienko, I. Shelykh, L. Gai, Z. Shen, D. Lidzey, P. Lagoudakis, *Commun. Phys.* **2020**, *3*, 1–10.

[18] A. V. Zasedatelev, A. V. Baranikov, D. Urbonas, F. Scafirimuto, U. Scherf, T. Stöferle, R. F. Mahrt and P. G. Lagoudakis, *Nat. Photonics* **2019**, *13*, 378–383.

[19] J. Tang, J. Zhang, Y. Lv, H. Wang, F. F. Xu, C. Zhang, L. Sun, J. Yao, Y. S. Zhao, *Nat. Commun*. **2021**, *12*, 3265.

[20] W. Ahn, F. Herrera, B. Simpkins, *Modification of Urethane Addition Reaction via Vibrational Strong Coupling*. ChemRxiv. Cambridge: Cambridge Open Engage, **2022**

[21] F. Herrera, J. Owrutsky, *J. Chem. Phys.* **2020**, *152*, 100902.

[22] D. Polak, R. Jayaprakash, T. P. Lyons, L. Á. Martínez-Martínez, A. Leventis, K. J. Fallon, H. Coulthard, D. G. Bossanyi ORCID logoa, Kyriacos Georgiou a, Anthony J. Petty, II a, John Anthony, H. Bronstein, J. Yuen-Zhou, A. I. Tartakovskii, J. Clark and A. J. Musser, *Chem. Sci.* **2020**, *11*, 343–354.

[23] L. A. Martínez-Martínez, M. Du, R. F. Ribeiro, S. Kéna-Cohen, J. Yuen-Zhou, *J. Phys. Chem. Lett.* **2018**, *9*, 1951–1957.

[24] E. Eizner, L. A. Martínez-Martínez, J. Yuen-Zhou, S. Kéna-Cohen, *Sci. Adv.* **2019**, *5*, 1–9.

[25] Y. Yu, S. Mallick, M. Wang, K. Börjesson, *Nat. Commun.* **2021**, *12*, 2–9.

[26] R. Pandya, A. Ashoka, K. Georgiou, J. Sung, R. Jayaprakash, S. Renken, L. Gai, Z. Shen, A. Rao, A. J. Musser, *Adv. Sci.* **2022**, *9*, 2105569.

[27] A. Thomas, L. Lethuillier-Karl, K. Nagarajan, R. M. A. Vergauwe, J. George, T. Chervy, A. Shalabney, E. Deveaux, C. Genet, J. Moran and T. W. Ebbesen, *Science* **2019**, *363*, 615–619.

[28] J. Galego, F. J. Garcia-Vidal, J. Feist, *Phys. Rev. X* **2015**, *5*, 041022.

[29] S. Kéna-Cohen, J. Yuen-Zhou, *ACS Cent. Sci.* **2019**, *5*, 386–388 (2019).

[30] M. Du, L. A. Martinez-Martinez, R. F. Ribeiro, Z. Hu, V. M. Menon, J. Yuen-Zhou, *Chem. Sci.* **2019**, *10*, 10821.

[31] D. M. Coles, N. Somaschi, P. Michetti, C. Clark, P. G. Lagoudakis, P. G. Savvidis and D. G. Lidzey, *Nat. Mater.* **2014**, *13*, 712–719.

[32] X. Zhong, T. Chervy, S. Wang, J. George, A. Thomas, J. A. Hutchison, E. Devaux, C. Genet, T. W. Ebbesen, *Angew. Chem.* **2016**, *55*, 6202–6206.

[33] X. Zhong, T. Chervy, L. Zhang, A. Thomas, J. George, C. Genet, J. A. Hutchison, T. W. Ebbesen, *Angew. Chem.* **2017**, *56*, 9034–9038 (2017).

[34] K. Georgiou, R. Jayaprakash, A. Othonos, D. G. Lidzey, *Angew. Chem.* **2021**, *133*, 16797-16803.

[35] C. Sánchez Muñoz, F. Nori, S. De Liberato, *Nat. Commun.* **2018**, *9*, 1924.

[36] T. Virgili, D. Coles, A. M. Adawi, C. Clark, P. Michetti, S. K. Rajendran, D. Brida, D. Polli, G. Cerullo, and D. G. Lidzey, *Phys. Rev. B* **2011**, *83*, 245309.

[37] S. Takahashi, K. Watanabe, Y. Matsumoto, *J. Chem. Phys.* **2019**, *151*.

[38] T. Schwartz, J. A. Hutchison, J. Léonard, C. Genet, S. Haacke, T. W. Ebbesen, *Chem. Phys. Chem.* **2013**, *14*, 125–131.

[39] C. A. DelPo, B. Kudisch, K. H. Park, S.-U.-Z. Khan, F. Fassioli, D. Fausti, B. P. Rand, and G. D. Scholes, *J. Phys. Chem. Lett.* **2020**, *11*, 2667–2674.

[40] A. G. Avramenko, A. S. Rury, *J. Phys. Chem. Lett.* **2020**, *11*, 1013–1021.

[41] G. G. Rozenman, K. Akulov, A. Golombek, T. Schwartz, *ACS Photonics* **2018**, *5*, 105–110.

[42] L. Mewes, M. Wang, R. A. Ingle, K. Börjesson, M. Chergui, *Commun. Phys.* **2020**, *3*, 157.

[43] J. M. Lüttgens, Z. Kuang, N. F. Zorn, T. Buckup, J. Zaumseil, *ACS Photonics* **2022**, *9*, 5, 1567–1576.

[44] S. Renken, R. Pandya, K. Georgiou, R. Jayaprakash, L. Gai, Z. Shen, D. G. Lidzey, A. Rao, A. J. Musser, *J. Chem. Phys.* **2021**, *155*, 154701.

[45] J. Keeling, S. Kéna-Cohen, *Annu. Rev. Phys. Chem.* **2020**, *71*, 435–459.

[46] V. M. Agranovich, M. Litinskaya, D. G. Lidzey, *Phys. Rev. B* **2003**, *67*, 085311.

[47] M. Litinskaya, P. Reineker, V. M. Agranovich, *J. Lumin*. **2004**, *110*, 364–372.

[48] E. Michail, K. Rashidi, B. Liu, G. He, V. M. Menon, M. Y. Sfeir, *Nano Lett.* **2024**, *24*, 557–565.

[49] S. Mukamel, *Annu. Rev. Phys. Chem.* **2000**, *51*, 691–729.

[50] D. M. Jonas, *Annu. Rev. Phys. Chem.* **2003**, *54*, 425–463.

[51] B. Xiang, R. F. Ribeiro, M. Du, L. Chen, Z. Yang, J. Wang, J. Yuen-Zhou, W. Xiong, *Science*, **2020**, *368*, 665-667.

[52] R. T. Allen, A. Dhavamani, M. Son, S. Kéna-Cohen, M. T. Zanni, M. S. Arnold, *J. Phys. Chem. C*, **2022**, *126*, 8417−8424.

[53] M. Son, Z. T. Armstrong, R. T. Allen, A. Dhavamani, M. S. Arnold, M. T. Zanni, *Nat. Commun.*, **2022**, *13*, 7305.

[54] G. G. Paschos, N. Somaschi, S. I. Tsintzos, D. Coles, J. L. Bricks, Z. Hatzopoulos, D. G. Lidzey, P. G. Lagoudakis and P. G. Savvidis, *Sci. Rep.* **2017**, *7*, 11377.

[55] R. Jayaprakash, K. Georgiou, H. Coulthard, A. Askitopoulos, S. K. Rajendran, D. M. Coles, A. J. Musser, J. Clark, I. D. W. Samuel, G. A. Turnbull, P. G. Lagoudakis and D. G. Lidzey, *Light Sci. Appl.* **2019**, *8*, 81.

[56] I. Stiopkin, T. Brixner, M. Yang, G. R. Fleming, *J. Phys. Chem. B* **2006**, *110*, 20032−20037.

[57] L. Luer, S. K. Rajendran, T. Stoll, L. Ganzer, J. Rehault, D. M. Coles, D. Lidzey, T. Virgili, G. Cerullo, *J. Phys. Chem. Lett.* **2017**, *8*, 547−552.

[58] R. Moca, S. R. Meech, I. A. Heisler. *J. Phys. Chem. B.* **2015**, *119*, 8623−8630.

[59] S. Richter, T. Michalsky, L. Fricke, C. Sturm, H. Franke, M. Grundmann, and R. Schmidt-Grund, *Appl. Phys. Lett*. **2015**, *107*, 231104.

[60] M. Balasubrahmaniyam, C. Genet, and T. Schwartz, *Phys. Rev. B* **2021**, *103*, L241407.

[61] K. Georgiou, K.E. McGhee, R. Jayaprakash, and D.G. Lidzey, *J. Chem. Phys*. **2021**, *154*, 124309.

[62] M. Godsi, A. Golombek, M. Balasubrahmaniyam, and T. Schwartz, *J. Chem. Phys*. **2023**, *159*, 134307.

[63] T. Virgili, D. G. Lidzey, D. D. C. Bradley, G. Cerullo, S. Stagira, and S. De Silvestri, *Appl. Phys. Lett.* **1999**, *74*, 2767.

[64] D.M. Coles, P. Michetti, C. Clark, W.C. Tsoi, A.M. Adawi, J.S. Kim, and D.G. Lidzey, *Adv. Funct. Mater.* **2011** *21*, 3691-3696.

[65] R.T. Grant, P. Michetti, A.J. Musser, P. Gregoire, T. Virgili, E. Vella, M. Cavazzini, K. Georgiou, F. Galeotti, C. Clark, J. Clark, C. Silva, and D.G. Lidzey, *Adv. Opt. Mater.* **2016** *4*, 1615-1623.

[66] K. Georgiou, R. Jayaprakash, A. Askitopoulos, D.M. Coles, P.G. Lagoudakis, and D.G. Lidzey, *ACS Photonics* **2018** *5*, 4343–4351.

[67] B. S. Simpkins, Z. Yang, A. D. Dunkelberger, I. Vurgaftman, J. C. Owrutsky, W. Xiong, *J. Phys. Chem. Lett.*, **2023**,*14*, 983-988.

[68] D. Timmer, M. Gittinger, T. Quenzel, S. Stephan, Y. Zhang, M. F. Schumacher, A. Lützen, M. Silies, S. Tretiak, J.-H. Zhong, A. De Sio, C. Lienau, *Nature Communications*, **2023**, *14*, 8035.

[69] T. Pajunpää ,F. Nigmatulin, S.-T. Akkanen, H. Fernandez, G. Groenhof, Z. Sun, *Physical Review B*, **2024**, *109*, 195409.

[70] J. Rehault; M. Maiuri; A. Oriana; G. Cerullo, *Rev. Sci. Instrum.* **2014**, *85*,1–10.

[71] D. Brida, C. Manzoni; G. Cerullo, *Optics Letters* **2012**, *37*, 3027–3029.

[72] T. Virgili, D. G. Lidzey, D. D. C. Bradley, S. Walker, *Synthetic Metals*, **2001**, *116*, 497-500.

[73] V. Butkus, D. Abramavicius, A. Gelzinis, L. Valkunas, *Lithuanian Journal of Physics* **2010**, *50*, 267-303.

[74] B. Xiang, R. F. Ribeiro, A. D. Dunkelberger, J. Wang, Y. Li, B. S. Simpkins, J. C. Owrutsky, J. Yuen-Zhou, W. Xiong, *Proc. Natl. Acad. Sci.* **2018**, *115*, 4845-4850.

[75] V.M.Agranovich and B.S.Toshich, *Sov. Phys. JETP* **1968**, *26*, 104-112.

[76] Y. Liu, F. Qin, Z.-Y. Wei, Q.-B. Meng, D.-Z. Zhang, and Z.-Y. Li, *Appl. Phys. Lett.* **2009**, *95*, 131116.

Table of contents:

Our work demonstrates how the strong light-matter coupling regime in an organic microcavity can be used to engineer energetic interactions between molecular films separated by several

microns. The quasi-instantaneous long-range electronic delocalization is driven by hybrid polaritonic states, as supported by a theoretical model. Our finding opens new perspectives on remote photo/induced energy transport useful in advanced optoelectronic devices.

M. Russo, K. Georgiou, A. Genco, S. De Liberato, G. Cerullo, D. G. Lidzey, A. Othonos, M. Maiuri*, T. Virgili*

Direct Evidence of Ultrafast Energy Delocalization Between Optically Hybridized J-Aggregates in a Strongly Coupled Microcavity

ToC figure

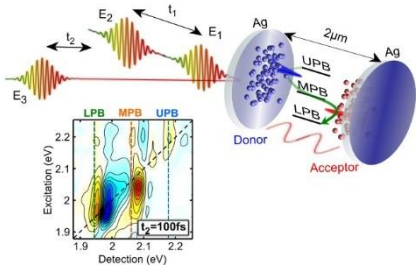

WILEY-VCH

Table of contents:

Our work demonstrates how the strong light-matter coupling regime in an organic microcavity can be used to engineer energetic interactions between molecular films separated by several microns. The quasi-instantaneous long-range electronic delocalization is driven by hybrid polaritonic states, as supported by a theoretical model. Our finding opens new perspectives on remote photo/induced energy transport useful in advanced optoelectronic devices.

M. Russo, K. Georgiou, A. Genco, S. De Liberato, G. Cerullo, D. G. Lidzey, A. Othonos, M. Maiuri*, T. Virgili*

Direct Evidence of Ultrafast Energy Delocalization Between Optically Hybridized J-Aggregates in a Strongly Coupled Microcavity

ToC figure